The present paper and previous work[4,5] have elaborated on the idea of kinetic and thermodynamic contributions to barriers of group-transfer reactions. The kinetic contribution $[\Delta E_0^{\ddagger}(1 - g_2)]$ is related to the intrinsic barrier and depends upon the barriers of two identity reactions,[1] while the thermodynamic contribution $[^1/_2\Delta E(1 + g_1)]$ derives from ΔE for the overall reaction. Both quantities can be obtained experimentally[2,5,31a] or computed quantum mechanically.[4,6] Equations 4 and 8 are compact ways of representing and predicting experimental data: n identity reactions provide sufficient information to calculate "intrinsic" barriers[1] for $n(n-1)/2$ unsymmetrical group-transfer reactions. It should be noted that for other classes of reactions (e.g., carbonyl additions, cycloadditions, fragmentations, electrocyclic reactions), the separation of barriers into kinetic and thermodynamic contributions is still useful, although the quantitative formalism is somewhat different.[56]

(55) For multistep reactions, other factors may be important. For discussion, see: (a) J. R. Murdoch and D. E. Magnoli, *J. Am. Chem. Soc.*, **104**, 2782 (1982). (b) W. P. Jencks, *Chem. Rev.*, **72**, 705 (1972).

Acknowledgment. This work was supported in part by a grant from the donors of the Petroleum Research Fund, administered by the American Chemical Society, by the Pennwalt Corporation Grant of Research Corporation, by a USPHS Biomedical Research Grant (4-521355-24739), by NSF, and by continued assistance from the University Research Committee (UCLA). J.R.M. also acknowledges a Regents' Junior Faculty Fellowship (1978-1979) and a UCLA Faculty Career Development Award (1979-1980). The author thanks Professor John Brauman and Drs. Mark Pellerite and Peter Ogilby for stimulating discussions and preprints.

(56) J. R. Murdoch, *J. Am. Chem. Soc.*, in press. The intrinsic barrier for any one-step reaction can be estimated from the Marcus equation by averaging the arithmetic and geometric means of the barriers in the forward and reverse directions. As the reaction approaches thermoneutrality, the arithmetic and geometric means converge and the intrinsic barrier is given by the average of the barriers for the forward and reverse directions. The intrinsic barrier from the Rehm-Weller equation corresponds to the geometric mean of forward and reverse barriers.

Paramagnetism and Antiaromaticity: Singlet-Triplet Equilibrium in Doubly Charged Benzenoid Polycyclic Systems

Abraham Minsky,[1a] Amatzya Y. Meyer,[1a] Raphael Poupko,[1b] and Mordecai Rabinovitz*[1a]

Contribution from the Department of Organic Chemistry, The Hebrew University of Jerusalem, Jerusalem 91904, Israel, and the Department of Isotope Research, The Weizmann Institute of Science, Rehovot 76100, Israel. *Received July 12, 1982*

Abstract: Fused benzenoid systems such as anthracene, phenanthrene, 3,4-benzophenanthrene, and chrysene were reduced with lithium, sodium, and potassium in various solvents to the antiaromatic doubly charged species. The NMR and ESR patterns of the dianions revealed a strong dependence on the countercation, solvent, and temperature. This dependence is interpreted by the existence of an equilibrium process between the singlet ground state and a thermally accessible excited triplet state of the antiaromatic dianions. The direction and extent of the equilibrium is determined by the energy gaps between the LUMO and HOMO of these charged species, which depends, in turn, on the topology of the hydrocarbon and on the solvation properties of the obtained salt.

Conjugated benzenoid polycyclic hydrocarbons undergo a 2-fold reduction process.[2] Scrutinized magnetic resonance studies, to be described below, performed on the resulting dianions reveal some hitherto unencountered phenomena that concern fundamental properties of antiaromatic charged systems. These phenomena point toward the existence of an equilibrium between the singlet ground state of the doubly charged benzenoid polycycles and a low-lying, thermally accessible excited triplet state. The equilibrium is found to have a substantial influence on the spectral patterns of these systems.

HMO considerations differentiate between two classes of $(4n + 2)$ π-conjugated polycyclic species: systems endowed with C_3 or higher axial symmetry for which the highest occupied and lowest unoccupied orbitals appear in pairs vs. systems with lower axial symmetry in which no such orbital degeneracies exist.[3] The difference between the two classes becomes crucial when the polycycles are reduced to the corresponding $(4n)$ π dianions. In the first group the two additional electrons populate two different degenerate orbitals, which may lead to a triplet ground state. This is the case in systems such as the triphenylene dianion (**1**),[4] 1,3,5-triphenylbenzene dianion (**2**),[5] and under strong solvating conditions the coronene dianion system (**3**).[6] It should be noted that dianions of C_3 or a higher symmetry do not adopt by necessity a triplet ground state. Calculations have shown that configuration

(1) (a) The Hebrew University of Jerusalem. (b) The Weizmann Institute of Science, Rehovot.

(2) (a) Streitwieser, A.; Suzuki, S. *Tetrahedron* **1961**, *16*, 153-168. (b) Cox, R. H.; Terry, H. W.; Harrison, L. W. *Tetrahedron Lett.* **1971**, *50*, 4815-4817. (c) For general review, see: Bates, R. B. In "Comprehensive Carbanion Chemistry"; Elsevier: New York, 1980; Part A, pp 1-54, and references cited therein.

(3) (a) Wert, J. E.; Bolton, J. R. "ESR Elementary Theory and Practical Applications"; McGraw-Hill: New York, 1972; pp 232-246. (b) Breslow, R. *Pure Appl. Chem.* **1982**, *54*, 927-938.

(4) (a) Willigen, H. v.; Broekhoven, J. A. M.; Boer, E. *Mol. Phys.* **1967**, *12*, 533-548. (b) Sommerdijk, J. L.; Boer, E. *J. Chem. Phys.* **1969**, *50*, 4771-4774.

(5) (a) Jesse, R. E.; Biloen, P.; Prins, R.; Voorst, J. D. W.; Hoijtink, G. J. *Mol. Phys.* **1963**, *6*, 633-635. (b) Broekhoven, J. A. M.; Sommerdijk, J. L.; Boer, E. *Ibid.* **1971**, *20*, 993-1003.

(6) (a) Glasbeek, M.; Voorst, J. D. W.; Hoijtink, G. J. *J. Chem. Phys.* **1966**, *45*, 1852. (b) Glasbeek, M.; Visser, A. J. W.; Maas, G. A.; Voorst, J. D. W.; Hoijtink, G. J. *Chem. Phys. Lett.* **1958**, *2*, 312-314.

0002-7863/83/1505-2164$01.50/0

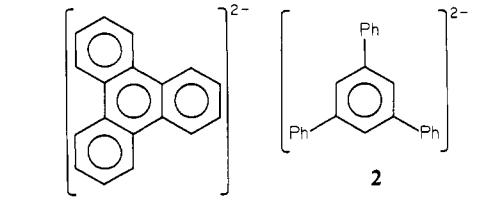

1

2

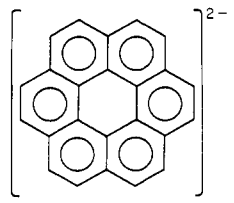

3

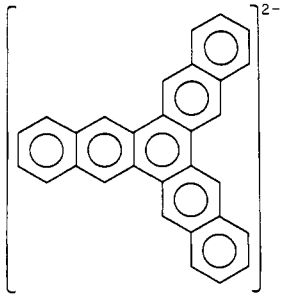

4

interaction could stabilize the singlet more than the corresponding triplet state.[3] This perhaps is the case in the trinaphthylene dianion system (**4**).[7]

Systems endowed with lower than 3-fold axial symmetry such as anthracene, phenanthrene, and chrysene form upon reduction dianions in which the singlet state is lower in energy than a triplet state. Here, the rigidity caused by the fused benzenoid skeleton requires planar or near planar geometry and, even more important, reduces substantially the extent of bond-length alternation. These consequences stand in obvious contrast with $(4n)$ π monocyclic conjugated species, which reveal very large deviations from a planar geometry and from constant or even nearly constant bond lengths.[8] As a result the LUMO–HOMO energy gap in doubly reduced benzenoid polycycles, with $(4n)$ π electrons in the path of conjugation, is much smaller than in monocyclic $(4n)$ π systems (and in the neutral $(4n + 2)$ π aromatic hydrocarbons). This is a point of great importance in understanding the observed properties of antiaromatic species (such as paramagnetic ring currents[9] and positive magnetic susceptibilities[10]) and serves as a pivot in the present work.

Results

The reduction of nine $(4n + 2)$ π-conjugated benzenoid hydrocarbons was conducted under various conditions, i.e., different reducing alkali metals and different solvents, and the NMR spectra of the charged products were studied at various temperatures. On the basis of the combined spectral data, the group of doubly charged benzenoid species can be differentiated into three clearly distinct subgroups. The three categories will now be described, each by means of a representative species. An interpretation of the spectral phenomena will then be presented and further illustrated by the other dianions.

Anthracene Dianion (5). The dianion of anthracene has been previously prepared by reduction of the hydrocarbon with lithium metal in tetrahydrofuran (THF), and its ^1H and ^{13}C NMR characteristics have been reported.[11] The ^1H NMR spectrum

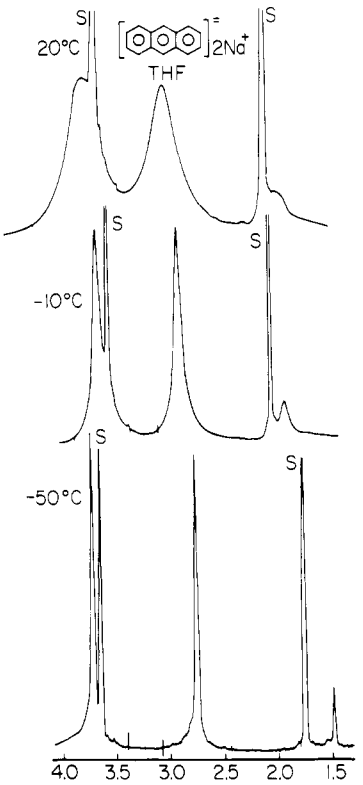

Figure 1. ^1H NMR spectrum of anthracene dianion (**5**) in THF at various temperatures. S refers to the solvent signals. See ref 27.

consists of an AA'BB' pattern at 4.25 and 3.36 ppm and a singlet at 1.80 ppm ($H_{2,3,6,7}$, $H_{1,4,5,8}$, and $H_{9,10}$; respectively). The sharp

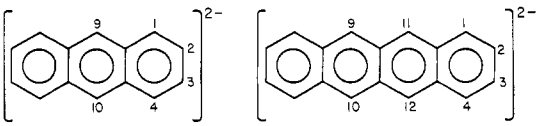

5 6

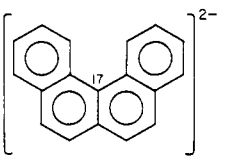

7

signals of the well-resolved spectrum indicate the existence of only minor extent of electron-exchange processes between the dianion and the corresponding monoanion radical (vide infra). We have studied the ^1H NMR chemical shifts of anthracene dilithium salt as function of temperature. In the range of temperatures between −60 °C and +40 °C, the spectrum remained unchanged. Neither could we detect any change in the ^{13}C NMR chemical shifts, which were identical with those already reported.[11b] The ^{13}C NMR absorptions remained sharp in the mentioned range of temperatures and clearly reflected the screening caused by the two negative charges.[13]

A different and rather unexpected situation occurs when sodium is used as the reducing agent. The ^1H NMR spectrum of anthracene disodium revealed a clear temperature dependence. At +40 °C no NMR absorptions could be detected. When the temperature was decreased to +20 °C, three very broad absorptions at ca. 3.85, 2.90, and 1.65 ppm (assigned to $H_{2,3,6,7}$, $H_{1,4,5,8}$, and $H_{9,10}$, respectively) appeared. As the temperature was gradually lowered, the signals became drastically sharper, yet even at −60 °C, the fine structure that is expected in an AA'BB' system

(7) Sommerdijk, J. L.; Boer, E.; Pijpers, F. W.; Willigen, H. v. *Z. Phys. Chem. (Wiesbaden)* **1969**, *63*, 183–189.
(8) Sondheimer, F., et al. *Spec. Publ.–Chem. Soc.* **1967**, *No. 21*, 75–107.
(9) (a) Mallion, R. B. *Pure Appl. Chem.* **1980**, *52*, 1541–1548. (b) Coulson, C. A.; Mallion, R. B. *J. Am. Chem. Soc.* **1976**, *98*, 592–598. (c) Pople, J. A.; Untch, K. G. *Ibid.* **1966**, *88*, 4811–4815. (d) Salem, L. "The Molecular Orbital Theory of Conjugated Systems"; Benjamin: New York, 1966; pp 194–196. (e) Haddon, R. C.; Haddon, V. R.; Jackman, L. M. *Fortschr. Chem. Forsch.* **1970**, *16*, 103–220. (f) Breslow, R. *Acc. Chem. Res.* **1973**, *6*, 393–398.
(10) (a) Van Vleck, J. H. "Electric and Magnetic Susceptibilities"; Oxford University Press: Oxford, England, 1932; pp 262–276. (b) Aihara, J. *J. Am. Chem. Soc.* **1979**, *101*, 558–563.
(11) (a) Lawler, R. G.; Ristagno, C. V. *J. Am. Chem. Soc.* **1969**, *91*, 1534–1535. (b) Mullen, K. *Helv. Chim. Acta* **1976**, *59*, 1357–1359.
(12) Netzel, T. L.; Rentzepis, P. M. *Chem. Phys. Lett.* **1974**, *29*, 337–342.
(13) Spiesecke, H.; Schneider, W. G. *Tetrahedron Lett.* **1961**, 468–471.

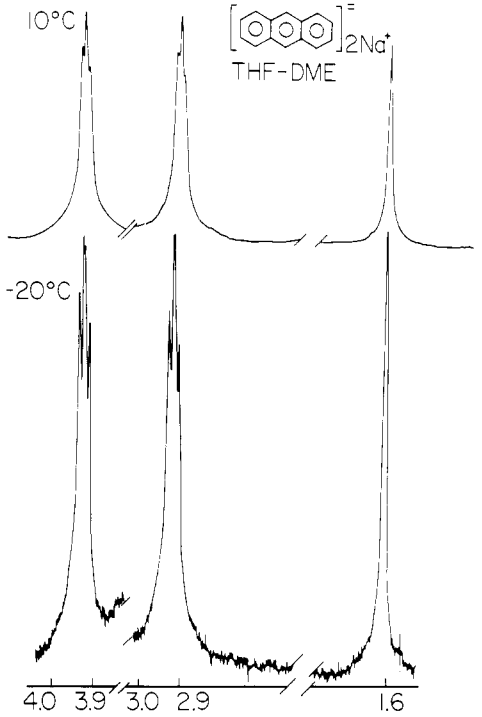

Figure 2. ^1H NMR spectrum (ppm, relative to $SiMe_4$) of anthracene dianion (**5**) in THF–DME (95:5) at various temperatures.

was not noticeable (Figure 1). The sharpening of NMR bands upon cooling was accompanied by a change in the color of the solution, from blue to dark blue-green. The changes in the line width of the absorptions and the color of the solution were both reversible, i.e., when the temperature was increased, the signals became broader and the color turned to blue, and then cooling showed again the above-described phenomena. We could not obtain the ^{13}C NMR of the dianion at ambient temperatures, and even at −30 °C the carbon spectrum gave a low signal-to-noise ratio.

A parallel experiment was conducted in a solution of tetrahydrofuran containing 5% dimethoxyethane (DME), a solvent of a high solvating power. At +20 °C the ^1H NMR signals were much sharper than those exhibited by anthracene disodium salt in pure tetrahydrofuran at the same temperature. Already at 0 °C a fine structure of the bands at 3.9 and 2.9 ppm was observed, and at −30 °C the spectrum revealed a well-resolved AA′BB′ pattern along with a narrow singlet at 1.64 ppm (Figure 2). The ^{13}C NMR bands at this temperature were similar to those exhibited by the anthracene dilithium salt. Here too, the changes in pattern as function of temperature were entirely reversible.

When the reduction was carried out with potassium metal (at −70 °C, THF), the dianion revealed no NMR spectrum peaks down to −20 °C. At lower temperatures, very broad absorptions at ca. 3.8, 2.9, and 1.6 ppm could be detected.

ESR measurement was carried out on a frozen THF solution (−120 °C) of the anthracene disodium system. The ESR spectrum of the dianion revealed a broad, unresolved line centered at ca. 3200 G, along with a sharp absorption at 1590 G. In the ESR spectrum of anthracene disodium in rigid 95:5 THF–DME, the low-field line could not be detected; the spectrum revealed only one, very broad absorption at 3200 G.

Tetracene Dianion (6). The ^1H NMR spectrum of tetracene disodium in THF was reported.[11a] The spectrum reveals an AA′BB′ pattern (4.85 ppm, $H_{2,3,6,7}$; 4.46 ppm, $H_{1,4,5,8}$) and a singlet (3.00 ppm, $H_{9,10,11,12}$). The dilithium[2b] and dipotassium[12] salts were obtained, but their ^1H NMR spectra were not reported. We repeated these experiments using lithium, sodium, and potassium as reducing agents. The ^1H and ^{13}C NMR spectra of the three salts in THF were studied as a function of temperature. Between −60 °C and +40 °C, no changes in spectral features were observed. The ^1H NMR lines of the three different systems remained sharp and well resolved. The ^{13}C NMR spectra consisted of four bands, their chemical shifts clearly reflecting the enhanced shielding due to two negative sharges,[13] and did not change with the reducing metal or the temperature. The ESR spectrum of tetracene disodium in frozen THF (−120 °C) revealed only one, broad band, at 3250 G.

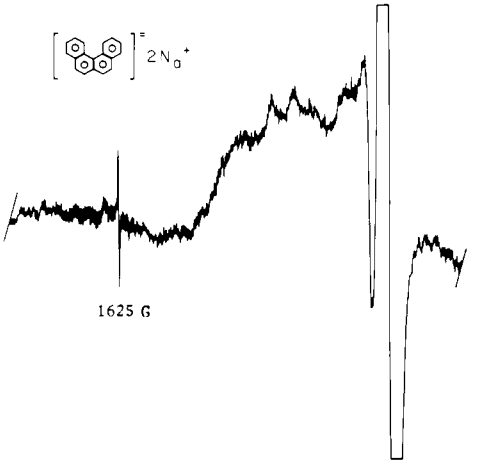

Figure 3. ESR spectrum of 3,4-benzophenanthrene dianion (**7**) in frozen solution (−120 °C) of THF.

3,4-Benzophenanthrene Dianion (7). The dianion of 3,4-benzophenanthrene was prepared by exposing THF or 95:5 THF–DME solutions of the neutral hydrocarbon to lithium,[2b] sodium, and potassium metals. In no case did the dianion reveal, between −70 °C and 30 °C, ^1H or ^{13}C NMR absorptions—even after 6 weeks of continuous exposure. ESR measurement was performed on the disodium species in frozen THF. The spectrum consisted of a broad absorption at 3200 G, along with a very sharp, intense signal at 1625 G (Figure 3).

Discussion

As mentioned, the three doubly charged systems illustrate three distinct categories of benzenoid dianions (Table II). The first subgroup, represented by the tetracene dianion system (**6**), includes doubly charged species that reveal highly resolved ^1H NMR spectra and sharp ^{13}C NMR bands. The NMR features of these dianions (chemical shifts, line shapes) are virtually independent of the reducing agent (Li, Na, or K), solvent, or temperature (in the range between −70 °C and +40 °C). Their ESR spectra in frozen THF reveal only one absorption, at ca. 3200 G. The second subgroup—exemplified by 3,4-benzophenanthrene dianion (**7**)—includes species that do not produce NMR spectra peaks irrespective of the experimental conditions. The ESR spectra of these dianions, as disodium in frozen THF, consist of two absorptions: a broad signal at 3200–3300 G, along with a strong, very sharp absorption at low field—1580–1620 G.

The most conspicuous and unexpected phenomena were revealed by the doubly charged species in the third subgroup, represented by the anthracene dianion system (**5**). The NMR spectra and the color exhibited by these salts showed a strong dependence upon the countercations, the solvents, and the temperature.

NMR Patterns. The factors that affect NMR features of charged conjugated polycyclic systems have been widely discussed.[14] Four such factors are known, namely, charge density, ring currents, the state of solvation of the salts, and the amount of paramagnetic radicals in the solution. Early in the development of NMR spectroscopy it was noticed that the chemical shift of an atom reflects the electron density in its vicinity. Empirically, it has been found that shielding of hydrogen or carbon atoms in charged conjugated systems varies linearly with the corresponding π-electron density ϕ. This led to an expression for the chemical shift $\Delta\sigma$ (with benzene or neutral starting material as references) of the form

(14) For a general review, see: Young, R. N. *Prog. Nucl. Magn. Reson. Spectrosc.* **1979**, *12*, 261–286.

$$\Delta\sigma = \alpha(\phi - 1)$$

where α is a positive constant that has been shown to equal approximately 10.7 or 180 ppm, for ^1H and ^{13}C chemical shifts, respectively.[13,15]

The concept of ring currents induced by external magnetic fields has been used to interpret a number of properties of conjugated cyclic molecules. Systems that are considered as aromatic according to Hückel's rule or to Platt's peripheral theory[16] sustain a diamagnetic ring current that causes a considerable downfield shift of nuclei located in the molecular plane outside the ring and an upfield shift—a shielding effect—inside. The diamagnetic ring current results from a cyclic delocalization of π-electron in the ground state of the systems. On the other hand, planar, conjugated species that are considered as antiaromatic by the mentioned theories reveal a paramagnetic ring current, caused by mixing low-lying excited electronic states with the ground state. As a result, the protons outside the ring undergo increased shielding and those inside are deshielded. The detection of such a type of ring current by means of NMR method is relatively simple, and their existence is taken as a qualitative criterion for aromatic or antiaromatic character.[9,17]

^1H and especially ^{13}C NMR chemical shifts have been used to characterize and study the equilibrium between contact and solvent-separated ion pairs. The various factors that determine the solvation properties are well established.[18] These factors include: (a) The nature of the alkali cation. (As the size of the cation increases (Li < Na < K), the equilibrium tends toward a tight contact ion.) (b) Increasing the temperature of the salt solution also favors intimate contact ion structure. (c) The solvating power of the solvent. Solvents endowed with strong solvating power (e.g., dimethoxyethane ≫ tetrahydrofuran > 2-methyltetrahydrofuran) favor a solvent-separated ion-pair structure. (d) The negative charge density in the organic moiety itself—a function of the size of the π system and the number of negative charges. A large charge density drives the equilibrium toward tight contact ions. Under conditions of tight contact ion pairs, the π-electron density is strongly polarized toward certain carbon atoms. As a result, these particular atoms are shielded and the others are deshielded relative to the chemical shifts of a solvent-separated salt. These effects are easily observed in ^{13}C NMR absorptions and, to a much lower extent, in ^1H NMR chemical shifts.

The presence of paramagnetic species such as radical anions and occurrence of electron-exchange processes between these species and diamagnetic compounds has a marked effect on NMR absorptions. The local field produced by the unpaired electron interacts with the magnetic moment of the nuclei, thus providing a very efficient mechanism for dipolar relaxation. The efficiency of this form of relaxation means that substantial NMR line broadening is produced even at low concentrations of the paramagnetic substance. Higher concentrations of the radical and efficient electron-exchange processes result in a total disappearance of NMR signals.[17b]

On these grounds, two interpretations of the NMR phenomena seem plausible at first sight. (a) Obviously, the observed line broadening—up to the total disappearance of signals—is strongly related to those factors that govern the ion solvation equilibrium. Spectra recorded at conditions that favor solvated ion pairs, that is, small countercations (Li vs. K), low temperature, and highly solvating media, exhibit sharp, resolved NMR signals. On the other hand, conditions in which contact ion pairing prevails result in line-broadening phenomena. An intimate ion-pair structure enhances the formation of large aggregates of the form $(R^{2-}, 2M^+)_n$[19] characterized by long correlation times for rotation. Correlation times longer than $\sim 10^{-9}$ s result in large T_1 relaxation times—a phenomenon of special significance under high spectrometer operating frequencies (e.g., 300 MHz).[20] Consequently, large countercations, high temperature, and solvents of relatively low solvating power are assumed to cause NMR line broadening and, hence, reduce signal intensities. (b) An alternative interpretation is based on the assumption that the equilibrium radical-anion ⇌ dianion is displaced to the right as K < Na < Li and to the left by raising the temperature. If so, when sodium or potassium is used and the salts are examined at a high temperature, the concentration of the paramagnetic radical-anion suffices to cause NMR line broadening.[17b]

Neither of these explanations stands further test. There is no reason to assume that species such as doubly charged anthracene, 3,4-benzophenanthrene (and phenanthrene, chrysene, etc., vide infra) would tend to form large aggregates with long correlation times and therefore inefficient T_1 relaxation mechanisms while systems of similar structure such as tetracene dianion would not. Furthermore, we have carried out the sodium reduction of anthracene in THF at two different hydrocarbon concentrations, viz., 10^{-1} M and 5×10^{-3} M. It is well-known that the concentration of the salt is of crucial importance in determining the extent of aggregate formation. Yet the spectral patterns of the two samples, as function of temperature, were identical. As to the second interpretation, lithium metal is indeed the stronger reducing agent in solvents of high dielectric constants such as water and to a lesser degree dimethylformamide (DMF). Yet this is due to the fact that the reducing ability of alkali metals in these media is dominated by the ion solvation energy, which is larger for Li^+ than for Na^+ or K^+. In etheral solvents, which are much poorer solvating media than water or DMF, the ionization energy factor, which varies as K > Na > Li, becomes crucial. Consequently, when potassium is used as reducing agent in THF, the equilibrium between the radical anions and dianions would shift toward the dianion to an extent higher than when the reduction is performed with lithium or sodium. Therefore, lower concentrations of line-broadening paramagnetic radical anions are expected. This argument is supported by experimental observations according to which potassium drives the reduction process faster and to a higher extent than lithium or sodium.[7,21]

Antiaromatic systems (defined as planar, $(4n)$ π-conjugated cyclic, or polycyclic, molecules with a low degree of bond length alternation) are characterized by a small LUMO–HOMO energy gap. If this gap is small enough to make the antibonding orbital thermally accessible, i.e., if an electron can be thermally lifted from the highest occupied to the lowest vacant orbital and then its spin reversed by some auxiliary mechanism, a low-lying excited triplet state can be produced.

We have performed Hückel MO calculations with variable β using the ω technique[22] on the doubly charged benzenoid systems. The calculations pointed toward an unequivocal relation between the spectral patterns of the so-defined antiaromatic species and their LUMO–HOMO energy gaps. The dinegative ions represented by the doubly charged tetracene (**6**), which produced highly resolved NMR spectra irrespective of countercation, solvent, and temperature, were all calculated to possess LUMO–HOMO energy gaps equal or larger than 0.4 β unit. Those doubly charged species, represented by 3,4-benzophenanthrene dianion (**7**) for which NMR spectra could not be observed under any conditions (second subgroup) revealed LUMO–HOMO energy gaps lower than 0.2 β unit. ESR spectra of these systems (in frozen THF solutions) were composed of a sharp low-field signal along with a broad line centered at ca. 3200 G. All the dinegative ions for which the energy gaps between the lowest unoccupied and the

(15) Schaefer, T.; Schneider, W. G. *Can. J. Chem.* **1963**, *41*, 966–982.
(16) Platt, J. R. J. *Chem. Phys.* **1954**, *22*, 1448–1458.
(17) (a) Emsley, J. W.; Feeney, J.; Sutcliffe, L. H. "High Resolution NMR Spectroscopy"; Pergamon Press; Oxford, England, 1965; Vol. 1. (b) Günther, H. "NMR Spectroscopy"; Wiley: New York, 1980; pp 218–220, 325–331.
(18) (a) O'Brien, D. H.; Russell, C. R.; Hart, A. J. *J. Am. Chem. Soc.* **1979**, *101*, 633–639. (b) Hogen-Esch, T. E.; Smid, J. *Ibid.* **1966**, *88*, 307–318.
(19) Hogen-Esch, T. E.; Smid, J. *Ibid.* **1967**, *89*, 2764–2765.
(20) Shaw, D. "Fourier Transform N.M.R. Spectroscopy"; Elsevier: New York, 1976; pp 297–309.
(21) Minsky, A.; Meyer, A. Y.; Rabinovitz, M. *J. Am. Chem. Soc.* **1982**, *104*, 2475–2482.
(22) Modified ω calculations on Coulomb and variable resonance integrals: (a) Berson, J. A.; Evleth, E. M.; Hamlet, Z. *J. Am. Chem. Soc.* **1965**, *87*, 2901–2908. (b) Boyd, G. V.; Singer, N. *Tetrahedron* **1966**, *22*, 3383–3392. (c) Streitwieser, A. *J. Am. Chem. Soc.* **1960**, *82*, 4123–4135.

highest occupied orbitals were estimated to range from 0.2 to 0.4 β unit, revealed NMR absorptions with line shapes highly dependent on countercation, temperature, and solvent. The systems in this third subgroup (represented by anthracene dianion (**5**)) exhibited sharp, low-field ESR lines, and as described in the anthracene disodium case, revealed a clear thermochromism.

On the basis of the narrow LUMO–HOMO energy gap in antiaromatic species and the observed relation between the values of these gaps and spectral patterns of the dinegative ions, *we propose the existence of an equilibrium process between a singlet ground state and a low-lying, thermally accessible triplet state in the doubly charged benzenoid systems.* The displacement toward the triplet is related to the energy difference between the lowest vacant and the highest occupied orbitals of the dinegative ion. In charged species with relatively large LUMO–HOMO gaps (>0.4 β), e.g., **6** (0.414 β), the equilibrium tends toward the singlet state, whereas in antiaromatic systems of small energy gaps (<0.2 β), e.g., **7** (0.111 β), large concentrations of the excited triplet state are obtained. These considerations lead to a straightforward interpretation of the NMR and ESR patterns exhibited by the first and second subgroups. In the first subgroup the main contribution to the magnetic susceptibility comes from paired, filled orbitals. Consequently, the NMR properties of these species are determined by a diamagnetic character produced by the closed shell. The obtained spectra are therefore highly resolved, and no line broadening is detected. In contrast, the narrow LUMO–HOMO gaps that characterize the dianions belonging to the second subgroup (e.g., 3,4-benzophenanthrene dianion) result in large population of the excited triplet state with two unpaired electrons. The strong interaction between the unpaired electron spins and the nuclear magnetic spins increases substantially the efficiency of nuclear dipolar relaxation mechanisms, shortening thus the relaxation times up to the point where no NMR signals can be detected (an identical effect is caused by the presence of monoradical species, vide supra).

The NMR spectra of the doubly charged systems in the third subgroup ($0.2 > \beta > 0.4$) reveal line-shape dependence upon the countercation, solvent, and temperature, i.e., those factors that determine the ion solvation equilibrium. NMR spectra recorded under conditions that favor highly solvated ion pairs, i.e., small countercations, low temperatures, and strongly solvating solvents, exhibit highly resolved patterns and sharp signals. In contrast, contact ion pairing results in line broadening up to a total disappearance of signals. To interpret this observation, we considered first-order perturbation[23] in the energy of a molecular orbital upon alteration of the Coulomb integral α at a given position. In Hückel-type calculations, this energy is given by

$$E_j = \sum_r C_{jr}^2 \alpha_r + 2\sum_r \sum_{s>r} C_{jr} C_{js} \beta_{rs}$$

where C_{jr} and C_{js} are the coefficients of the atomic orbitals r and s in the jth molecular orbital. When the Coulomb integral at a given position p is altered while leaving all other integrals ($\alpha_{r\neq p}$, β_{rs}) unchanged, the energy of the molecular orbital j is modified,

$$\delta E_j = C_{jp}^2 \delta\alpha_p$$

Displacement of the solvation equilibrium, from solvated to intimate ion pairs, implies that a metal cation approaches closely some position p on the charged hydrocarbon. This produces an accumulation of negative charge at p, which accordingly becomes less electronegative, $\alpha_p = \alpha_p^0 - h\beta$ ($h > 0$, $\beta < 0$). Hence,

$$\delta E_j = C_{jp}^2 \delta\alpha_p = -C_{jp}^2 h\beta$$

In this case h reflects the proximity of the metal cation to the carbon skeleton, and it is evident that the energy change depends on the magnitude of C_{jp}. When the atomic orbital coefficients in the HOMO and LUMO of the doubly charged benzenoid systems are inspected ($\omega\beta$ method), an unequivocal regularity is repeatedly observed: those carbon atoms that bear the highest overall electron density and are therefore expected to be closer to the cations than other carbons in the organic moiety, correspond to large atomic coefficients in the HOMO and to very small coefficients in the LUMO (Table I). Consequently, when contact ion pairs prevail, the energy of the highest occupied molecular orbital increases to a greater extent than that of the lowest vacant orbital, and therefore the LUMO–HOMO energy gap decreases. As a result, conditions favoring contact ions shift the singlet–triplet equilibrium toward the excited triplet and causes NMR line broadening and even a total signal disappearance. It should be noted, however, that this treatment is somewhat simplified and that more sophisticated calculations should be carried out in order to specify more rigorously the role of the countercation. When the initial LUMO–HOMO gaps are relatively wide (first subgroup) or relatively narrow (second subgroup), the energy changes do not suffice to produce any fundamental alteration in the NMR spectral patterns. Only for species of the intermediate type such as anthracene dianion (third subgroup) are the NMR patterns sensitive to modifications that are caused by shift of the solvation equilibrium.

Table I. HOMO and LUMO Atomic Orbital Coefficients of Carbons Bearing the Highest Charge Density in the Dianions

dianions	carbons of highest charge density[a] (denoted as P carbons)	atomic orbital coefficient[b] of P carbons: in the dianion's HOMO	atomic orbital coefficient[b] of P carbons: in the dianion's LUMO
anthracene (**5**)	9 (10)	0.4360	0.0000
3,4-benzophenanthrene (**7**)	17	0.3846	0.0000
1,2,3,4-dibenzanthracene (**9**)	9 (10)	0.3851	0.1170
phenanthrene (**10**)	9 (10)	0.3749	0.1280
chrysene (**11**)	2 (8)	0.3819	0.0442
1,2-benzanthracene (**12**)	7	0.4331	0.0924
1,2,5,6-dibenzanthracene (**13**)	7 (14)	0.3195	0.2580

[a] For numbering, see text. [b] Absolute value–obtained by $\omega\beta$ calculations.[22]

ESR Patterns. Early attempts to detect ESR absorptions of triplet ground state and, in particular, thermally or photoexcited triplet state for randomly oriented molecules were not successful, mainly because of the large spin–spin interaction between the two unpaired electrons, which is markedly anisotropic.[3a,24] The splitting of the three spin functions of the triplet state due to this anisotropic dipolar interaction is uneven and depends strongly on the orientation of the principal axes of the molecule with respect to the magnetic field. The first successful detection of triplet-state ESR was that of oriented phosphorescent naphthalene in substitution sites in a single crystal of durene.[24] The signals that were observed are due to the first-order transitions, ($\Delta M_s = \pm 1$) between spin eigenfunctions that correspond to the quantum numbers $M_s = -1, 0, +1$. Along with them, second-order "forbidden" transition ($\Delta M_s = 2$) could be observed at low magnetic fields, coined as "half-field" transition. At low field, the spin functions become linear combinations of the high-field states, and therefore the usual $\Delta M_s = \pm 1$ selection rule does not apply. More difficult by far is the detection of ESR absorptions of randomly oriented systems in the triplet state. It is virtually impossible to obtain ESR spectra of triplet-state species in nonrigid media. Molecular reorientation in fluid solutions results in a rapid rate modulation of intramolecular spin–spin interactions. These modulations lead to very short spin lifetimes and consequently to undetectably broad lines. In a rigid, nonoriented matrix, $\Delta M_s = \pm 1$ transitions are smeared over a large-field range due to the mentioned strong spin–spin interaction anisotropy. In contrast, $\Delta M_s = 2$ transitions are characterized by small anisotropy, and therefore the absorptions associated with these transitions would be much sharper than those associated with $\Delta M_s = 1$ transitions.[3a,24] Hence, the

(23) Dewar, M. J. S. "The Molecular Orbital Theory of Organic Chemistry"; McGraw-Hill: New York, 1969; pp 194–199.

(24) (a) Hutchison, C. A.; Magnum, B. W. *J. Chem. Phys.* **1961**, *34*, 908–916. (b) Gordy, W. "Theory and Applications of ESR" Wiley: New York, 1979; pp 551–557.

Table II. Spectral Patterns and LUMO–HOMO Energy Gaps of the Three Subgroups of Doubly Charged Systems

doubly charged systems	LUMO–HOMO gap,[a] β-units	^{1}H NMR patterns[b] 30 °C	−20 °C	−60 °C	ESR patterns, half-field line[c]
tetracene-Li/THF	0.414	C	C	C	
-Na/THF		C	C	C	N
9,10-diphenylanthracene-Na/THF	0.420	C	C	C	N
anthracene-Li/THF	0.310	C	C	C	
-Na/THF		-	A	B	1590
-Na/THF-DME		B	C	C	N
-K/THF		-	-	A	
chrysene-Li/THF	0.272	B	C	C	
-Na/THF		-	A	B	1620
1,2,5,6-dibenzanthracene-Li/THF	0.251	B	C	C	
-Na/THF		-	A	C	N
1,2-benzanthracene-Li/THF	0.226	A	C	C	
-Na/THF		-	-	A	1600
phenanthrene-Li/THF	0.231	-	A	A	
-Li/THF-DME		-	A	B	
-Na/THF		-	-	-	1595
1,2,3,4-dibenzanthracene-Li/THF	0.157	-	-	-	
-Na/THF		-	-	-	1605
3,4-benzophenanthrene-Li/THF	0.111	-	-	-	
-Na/THF		-	-	-	1625

[a] Obtained by $\omega\beta$ calculations.[22] [b] (-) No spectra obtained; (A) broad lines, unresolved structure; (B) sharp lines, unresolved structure, (C) sharp lines, fine resolved structure. [c] (N) No half-field signal. When half-field absorption is detected, its field is given in gauss.

detection of a $\Delta M_s = 2$ transition in a nonoriented rigid solution is by far easier than the detection of $\Delta M_s = \pm 1$ signals.

The ESR spectra of dinegative ions derived from tetracene, 3,4-benzophenanthrene, and anthracene, as well as from all the other benzenoid polycycles, were recorded in frozen, rigid THF solutions. Comparison between the spectral patterns of charged species belonging to the second and third subgroups and those patterns obtained from the first reveals a pronounced dissimilarity. While the latter exhibit only one broad, unresolved absorption at ca. 3200 G, assigned to the monoanion radical (doublet) species, all the former systems exhibit an additional very sharp, low-field signal (Table II). On the grounds of the above discussion, the low-field line is assigned to the $M_s = 2$ transition of a thermally accessible excited triplet state in equilibrium with the ground singlet. ESR spectra of thermally excited triplet of randomly oriented molecules in frozen solutions are documented. The coronene[6] and 2,4,6-triphenyl-*sym*-triazine[5b] dinegative ions reveal half and normal field ESR patterns characteristic of randomly oriented species in triplet state. The ESR signal intensities of the two systems exhibit clear temperature dependence—as expected for a thermally excited triplet.

Up to now, we were not able to obtain in our doubly charged systems the "normal" field absorptions. The half-field signals were easily obtained and a study of these absorptions dependence on temperature is in progress.

The observed thermochromism encountered in anthracene disodium–THF and in other systems that belong to the third subgroup might also be interpreted in terms of a singlet–triplet equilibrium. The reversible change of color with temperature, in those systems where the singlet–triplet equilibrium is solvation dependent, is explained as due to the difference in population at the two states. Obviously, the excited triplet state, prevailing at elevated temperatures, has its own characteristic electronic absorptions, as does the singlet ground state observed at lower temperatures. The phenomenon of thermochromism due to the alternation of singlet–triplet population was observed in other systems such as dianthrone-2,2′-dicarboxylic acid.[25]

The dinegative ions of tetracene (**6**), 3,4-benzophenanthrene (**7**) and anthracene (**5**) were chosen to represent the three subgroups of doubly charged benzenoid systems. We have studied the spectral patterns of six other dianions and find that they strongly support the singlet–triplet equilibrium interpretation (Table II).

(25) Grubb, W. T.; Kistiakowsky, G. B. *J. Am. Chem. Soc.* **1950**, *72*, 419–424.

9,10-Diphenylanthracene Dianion (8). The reduction of 9,10-diphenylanthracene was carried out by using Li and Na metals as reducing agents in THF. The purple solution of the obtained

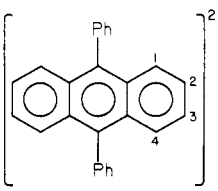

8

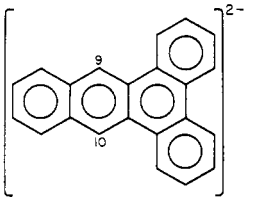

9

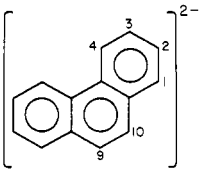

10

dianion revealed a well-resolved ^{1}H NMR spectrum (6.5–7 ppm, phenyl protons; 3.8 and 4.1 ppm, two parts of an AA′BB′ patterns $H_{1,4}$ and $H_{2,3}$, respectively) along with sharp ^{13}C NMR absorptions. Spectral patterns were identical with Na^+ or Li^+ as countercations and remained unchanged when the temperature was varied between −60 °C and +30 °C. No "half-field" absorptions could be detected in the ESR spectrum of **8** as the disodium salt in glassy THF solution. The estimated LUMO–HOMO energy gap of the dianion is 0.420 β—a relatively large value that points to very small concentrations, if any, of ions in the excited triplet state. Thus, 9,10-diphenylanthracene belongs to the first subgroup.

1,2,3,4-Dibenzanthracene Dianion (9). The LUMO–HOMO energy gap of **9** is estimated to be 0.157 β unit. This system is thus expected to belong to the second subgroup, with a large concentration of the triplet state in the singlet–triplet equilibrium. In fact, no NMR absorptions were exhibited by **9**, irrespective of counterion (Li^+ and Na^+), solvent (THF or 95:5 DME–THF), and temperature. The ESR spectrum of **9** as the disodium salt in frozen THF solution (−120 °C) revealed a sharp, intense "half-field" signal at 1605 G, assigned to the $\Delta M_s = 2$ transition, along with a broad radical-anion transition at ca. 3200 G.

Phenanthrene Dianion (10). Sodium or potassium reduction of phenanthrene in THF or in THF containing 5% DME did not afford any NMR signals at the temperature range −80 °C to +40

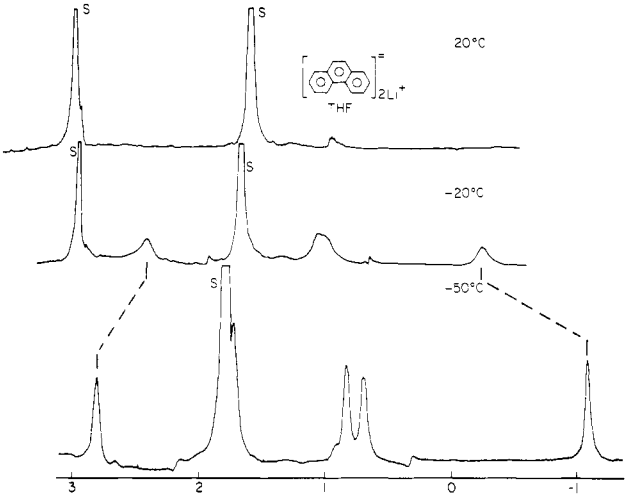

Figure 4. ^{1}H NMR spectrum of phenanthrene dianion (**10**) in THF at various temperatures. S refers to the solvent signals. See ref 27.

°C. ESR spectrum of **10** as the disodium salt in rigid solution of THF (−120 °C) revealed a sharp low-field signal (Figure 4). However, lithium reduction resulted in very broad, high-field ^{1}H NMR absorptions that appeared at −30 °C. Further cooling caused line narrowing, yet no highly resolved spectrum could be obtained (Figure 5). Conducting the experiment in 95:5 THF–DME resulted in further line sharpening. The chemical shifts were similar to those already reported[26] (0.5 ppm, $H_{1,8}$; 2.7 ppm, $H_{2,7}$; 1.6 ppm, $H_{3,6}$; 0.7, ppm $H_{4,5}$; −1.9 ppm, $H_{9,10}$). A clear reversibility of NMR line shapes as function of temperature was observed.

The LUMO–HOMO gap of **10** is found to be 0.231 β. In view of this gap and of the solvation-dependent spectrum, the dinegative ion of phenanthrene is assigned to the third subgroup.

Chrysene Dianion (11). The doubly charged chrysene as the disodium salt in THF at +20 °C did not reveal NMR patterns.

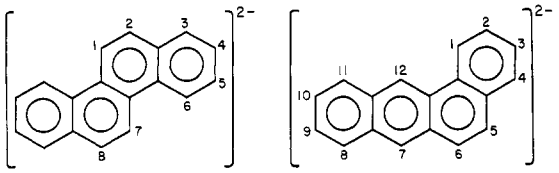

11

12

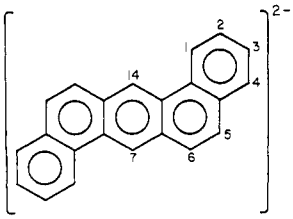

13

As the temperature was decreased to −50 °C, broad absorptions appeared; further decrease of temperature caused line narrowing (Figure 6). No fine structure was obtained even as low as −80 °C. The sharpening of the NMR bands upon cooling was accompanied by a change in the color of the dianion solution from purple-blue to green. Both the change in NMR line width and the change of color were reversible as function of temperature.

The ESR spectrum of **11** as the disodium salt (THF, −120 °C) exhibited a strong "half-field" signal at 1620 G along with the broad "normal" absorption at 3200 G.

(26) Müllen, K. *Helv. Chim. Acta* **1978**, *61*, 1296–1304.

(27) The scale (ppm, relative to $SiMe_4$) refers to the spectrum recorded at the lowest temperature. This spectrum was enlarged relative to the other spectra to emphasize the line-sharpening process and the highly resolved patterns.

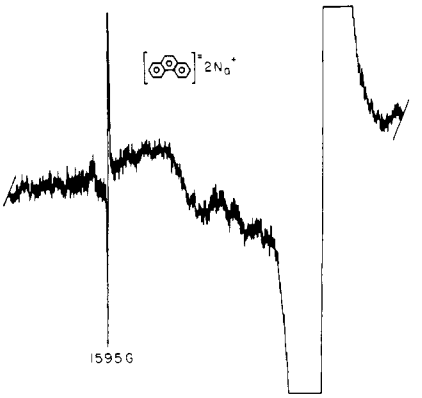

Figure 5. ESR spectrum of phenanthrene dianion (**10**) in frozen solution (−120 °C) of THF.

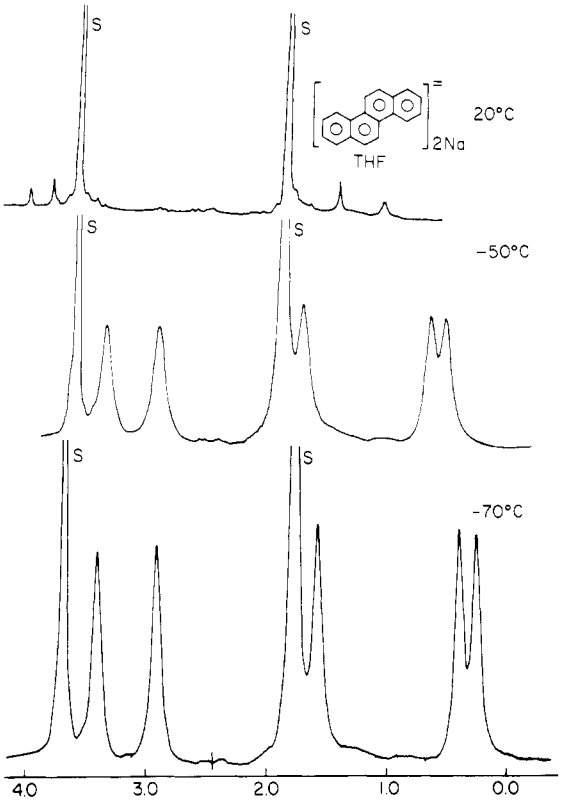

Figure 6. ^{1}H NMR spectrum of chrysene dianion (**11**) as disodium salt in THF at various temperatures. S refers to the solvent signals. See ref 27.

When the reduction of chrysene was carried out with lithium metal, ^{1}H NMR broad lines were observed even at room temperature. As the temperature was gradually lowered, a drastic line narrowing took place, and at −40 °C a sharp, highly resolved ^{1}H NMR spectrum was obtained (0.9 ppm, H_2, d; 1.2 ppm, H_1, d; 2.5 ppm, $H_{4,5}$, dd; 3.5 ppm, H_3, t; 3.9 ppm, H_6, t (Figure 7)). Increasing the temperature caused line broadening.

The LUMO–HOMO energy gap of **11** is 0.273 β. Accordingly, the system is expected to reveal triplet concentrations as a function of solvation-ion equilibrium, which indeed it does.

1,2-Benzanthracene Dianion (12). The LUMO–HOMO gap in **1** is estimated as 0.225 β, close to the value revealed by the phenanthrene dianion. Indeed, the spectral patterns as a function of solvation factors are much the same. No NMR spectrum is obtained from 1,2-benzanthracene dianion as the disodium salt in THF or in 95:5 THF–DME irrespective of temperature. the ESR spectrum revealed a "half-field" band at 1600 G. As the dlithium salt, the blue-green solution of **12** exhibited very broad lines at room temperature and even at −20 °C a well-resolved ^{1}H NMR spectrum was obtained (4.85 ppm, $H_{1,2,3,4}$, center of

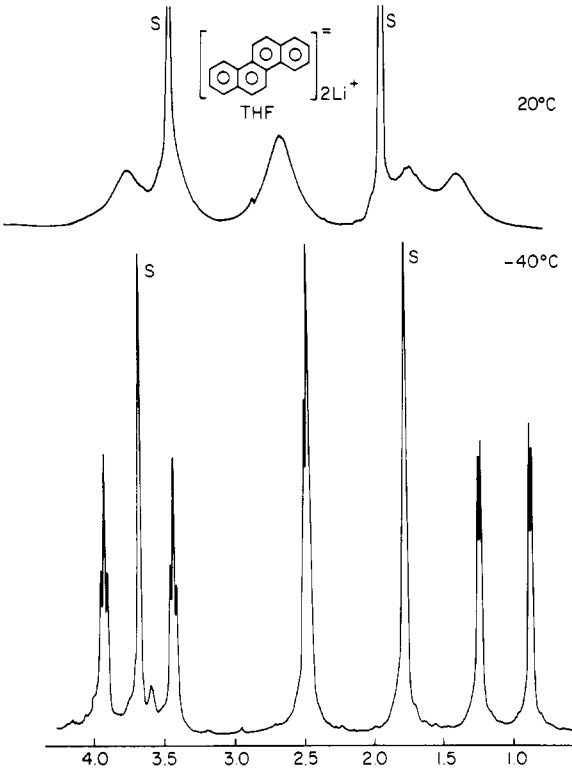

Figure 7. ^{1}H NMR spectrum of chrysene dianion (**11**) as dilithium salt in THF at various temperatures. S refers to the solvent signals. See ref 27.

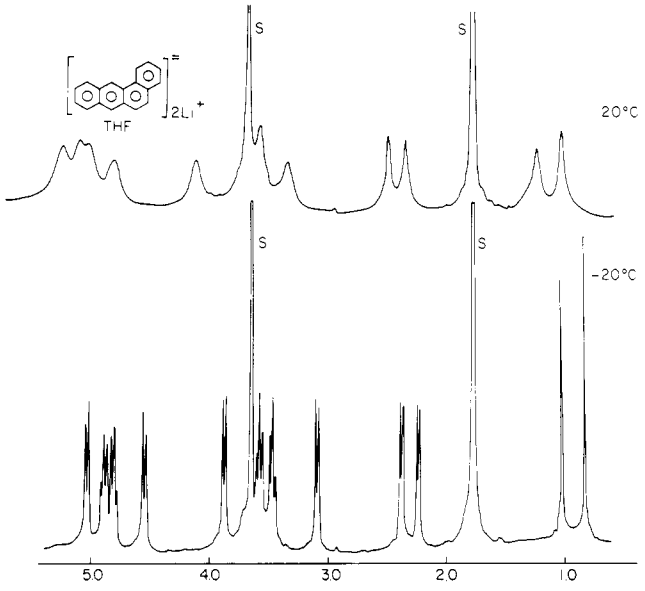

Figure 8. ^{1}H NMR spectrum (ppm, relative to $SiMe_4$) of 1,2-benzanthracene dianion (**12**) as dilithium salt in THF at various temperatures. S refers to the solvent signals.

multiplet; 3.55 ppm, $H_{8,9,10,11}$, center of multiplet; 2.39 ppm, H_6, d; 2.25 ppm, H_5, d; 1.05 ppm, H_{12}, s; 0.85 ppm, H_7, s (Figure 8)).

1,2,5,6-Dibenzanthracene Dianion (13). The blue solution of **13** as the disodium salt did not reveal ^{1}H NMR absorptions at room temperature. Cooling to −20 °C led to the appearance of broad signals, and at −50 °C a well-resolved spectrum was obtained (2.77 ppm, H_2, t; 3.56 ppm, H_3, t; 3.27 ppm, H_4, d; 1.98 ppm, H_5, d; 1.53 ppm, H_1, d; 0.36 ppm, H_6, d; −2.15 ppm, H_7, s (Figure 9)). The gradual lowering of temperature was accompanied by a drastic change in the color of the solution from blue to dark green-brown. The NMR line-shape changes as well as the color alterations showed a clear reversibility as a function of temperature. The ^{1}H NMR spectrum of **13** as the dilithium salt revealed sharp, well-resolved absorptions even at 0 °C. The ESR spectrum

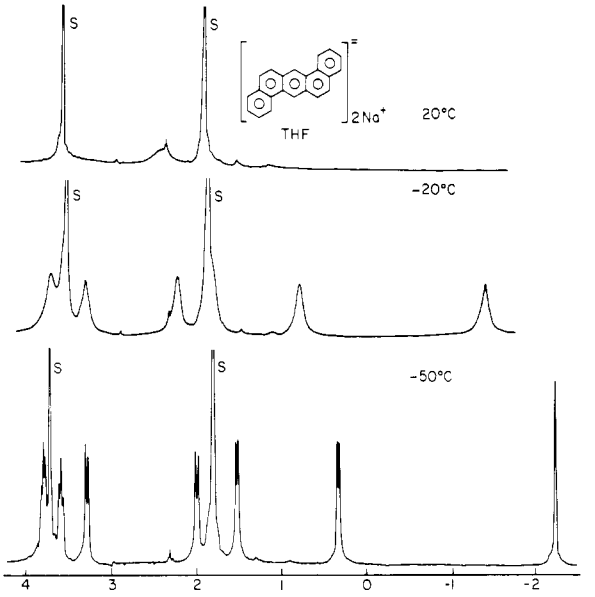

Figure 9. ^{1}H NMR spectrum of 1,2,5,6-dibenzanthracene (**13**) in THF at various temperatures. S refers to the solvent signals. See ref 27.

of **13** (as disodium salt in frozen, rigid THF solution) revealed only the broad, unresolved line assigned to the monoradical anion.

The estimated LUMO–HOMO gap in **13** is 0.252 β. This value still accords with singlet–triplet equilibrium but to an extent lower than in other dianions in the third subgroup. Up to now only three out of four factors mentioned to dominate the ion-solvation equilibrium were shown to influence the singlet–triplet equilibrium, namely, the countercation, the solvent, and the temperature. The spectral patterns of **10**, **12**, and **13** emphasize now the role of the fourth factor, i.e., the charge density. The LUMO–HOMO energy gaps in these three doubly charged systems are very similar, yet the spectral patterns are different. Phenanthrene dilithium (**10**) did not reveal a sharp, well-resolved ^{1}H NMR spectrum even at −70 °C. 1,2-Benzanthracene dilithium (**12**) exhibited well-resolved ^{1}H NMR patterns at −20 °C, yet did not afford NMR absorptions when Na was used as reducing agent. The 1,2,5,6-dibenzanthracene dianion, as dilithium, revealed a highly resolved spectrum even at 0 °C. Charge densities in **13** (two negative charges spread over five benzenoid rings) are smaller than those in **12** (four rings), which are still smaller than those in **10**. Consequently, the ion-solvation equilibrium in **10** tends more toward a tight contact ion than in **12** and in **13**. Hence the effect of decreasing the LUMO–HOMO energy gap due to tight contact pairing (vide supra) is much more pronounced in phenanthrene dianion (**10**) than in 1,2-benzanthracene dianion (**12**); in the dinegative ion of 1,2,5,6-dibenzanthracene, the LUMO–HOMO gap narrowing effect due to intimate contact ions is even smaller. Larger concentrations of systems in a thermally accessible triplet state are therefore expected, and observed, in **10** more than in **12** or in **13**.

Conclusions

The existence of an equilibrium process between singlet ground state and a low-lying, thermally accessible, triplet state is revealed in doubly charged benzenoid ($4n$) π systems. The extent and direction of this equilibrium is determined solely by the width of the energy gap between the lowest vacant and the highest occupied molecular orbitals of the dianion. The gap's width depends in turn on the topology of the hydrocarbon and on the solvation properties of the obtained salt.

As to the topology, when the energy gaps are relatively large, no contribution to an excited triplet is expected. A closed electronic shell is obtained and consequently sharp, well-resolved diamagnetic NMR patterns are exhibited. In contrast, when the LUMO–HOMO gap is estimated narrow, the triplet concentration is large, causing very fast nuclear relaxations and disappearance of NMR signals. A half-field absorption—highly characteristic to triplet

state—appears in the ESR spectra of these dianions. When intermediate gap values are estimated, ion solvation determines the extent of singlet–triplet equilibrium via further alteration of the energy gap. In such cases the dependence of NMR line shape upon solvation factors is observed.

The present study points toward an obvious relation between NMR and ESR spectral data on the one hand and LUMO–HOMO energy separation on the other and therefore emphasizes the connection between antiaromaticity and paramagnetism. Even more so, it suggests the possibility of using the LUMO–HOMO gap, as obtained by simple $\omega\beta$ calculations, for predicting chemical and physical properties of antiaromatic species and even for preliminary estimation of the extent of antiaromatic character of $(4n)$ π conjugated systems.[9f]

Experimental Section

The benzenoid hydrocarbons were purchased from Aldrich Company and recrystallized before use from EtOH (anthracene, phenanthrene, and 9,10-diphenylanthracene) or from toluene (all other hydrocarbons).

General Procedure for the Metal Reduction Process. A wire of lithium, sodium, or potassium was introduced to the upper part of an extended tube. For NMR measurements, 5-mm tubes were used, containing 10^{-2} M (unless otherwise stated in the text) of the hydrocarbon dissolved in 0.8 mL of THF-d_8 (Aldrich reagent). For ESR measurements, 3-mm o.d. quartz tubes containing 10^{-3} M of the hydrocarbon in THF solution were used. The frozen solution of the hydrocarbon was degassed, and then the tube was sealed under vacuum. By turning the tube, the solution was brought into contact with the metal wire for controlled periods of time.

The NMR spectra were obtained on Bruker WH-300 pulsed FT spectrometer operating at 300.133 MHz and 75.46 MHz for ^1H and ^{13}C, respectively. The field/frequency regulations were maintained by locking to the solvent deuterium. The free induction decay signals were digitized and accumulated on an Aspect-2000 computer (32 K).

The ESR spectra were recorded on a Varian E-3 ESR spectrometer (X-band frequency) and a Varian E-257 variable-temperature unit. Long (30-min) sweep times were essential due to the narrowness of the half-field absorptions.

Registry No. 5, 56481-92-6; **5**·2Li, 39399-94-5; **5**·2Na, 11065-56-8; **5**·2K, 39399-93-4; **6**, 53571-97-4; **6**·2Li, 58054-37-8; **6**·2Na, 11067-61-1; **6**·2K, 55573-89-2; **7**, 78850-97-2; **7**·2Na, 84809-94-9; **7**·2K, 58054-36-7; **7**·2Li, 84809-96-1; **8**, 78851-99-7; **8**·2Li, 84809-98-3; **8**·2Na, 84810-00-4; **9**, 78850-93-8; **9**·2Li, 84810-02-6; **9**·2Na, 84810-04-8; **10**, 67382-15-4; **10**·2Na, 84810-06-0; **10**·2K, 84810-08-2; **10**·2Li, 54667-02-6; **11**, 78850-96-1; **11**·2Na, 83831-05-4; **11**·2Li, 83831-06-5; **12**, 78858-01-2; **12**·2Na, 84810-10-6; **12**·2Li, 84810-11-7; **13**, 78850-92-7; **13**·2Na, 84810-13-9; **13**·2Li, 84823-77-8.

Intramolecular Orbital Interactions in Triptycene Studied by Photoelectron Spectroscopy

Tsunetoshi Kobayashi,*[1a] Tanekazu Kubota,[1b] and Kiyoshi Ezumi[1c]

Contribution from the Institute of Physical and Chemical Research, Wako, Saitama 351, Japan, Institute for Solid State Physics, the University of Tokyo, Roppongi, Minato, Tokyo 106, Japan, Gifu College of Pharmacy, Mitahora-higashi, Gifu 502, Japan, and Shionogi Research Laboratories, Shionogi and Co., Ltd., Fukushima, Osaka 553, Japan. *Received June 28, 1982*

Abstract: In order to make clear the relative roles of through-space and through-bond orbital interactions in triptycene, its vapor-phase He I photoelectron spectrum was measured. A simple LCBO through-space interaction model calculation reproduced almost quantitatively the principal feature of the observed overall spectral pattern for the first two band groups. This fact suggests that the through-space interactions among the benzene ring e_{1g}-like group π orbitals are dominating as for the first six HO-π-MOs, the effect of through-bond interactions being negligibly small in contrast to the case of barrelene.

Triptycene (9,10-dihydro-9,10[1′,2′]benzenoanthracene, **1**) is

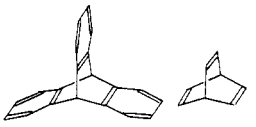

1 2

a molecule of high symmetry (D_{3h})[2-4] containing three benzene rings equivalent to one another as its constituents and is one of the fundamentally important systems, along with barrelene (bicyclo[2.2.2]octa-2,5,7-triene, **2**), from the standpoint of intramolecular orbital interactions. The primary interest at the present time is the relative roles of through-space and through-bond[5] interactions among the π-electron systems of the three benzene rings in **1**. In this paper, **1** is studied by photoelectron (PE) spectroscopy, which is a very powerful tool for investigating the occupied MOs, and the intramolecular interactions among the six e_{1g}-like group π orbitals of the three benzene rings in **1** are discussed on the basis of a simple LCBO model consideration.

Concerning compound **2**, closely related to but much simpler than **1**, Haselbach et al.[6] discussed the interactions among the three olefinic-group occupied π orbitals based on its PE spectrum,

Table I. Experimental Vertical Ionization Energies, IE_v

compound	IE_v, eV
triptycene (1)	7.98, 8.80,[a] 9.16,[a] 10.71
o-xylene[b]	8.75, 9.0, 11.25
barrelene (2)[c]	8.23, 9.65,[d] 10.02,[d] 11.25
propene[e]	9.73, 12.2
cis-2-butene[e]	9.12, 11.7

[a] Apparent band maxima in the highly overlapping region. [b] Reference 13. [c] Reference 6. [d] The Jahn-Teller split-band maxima. [e] Reference 14.

(1) (a) Institute of Physical and Chemical Research and University of Tokyo. Address correspondence to Institute of Physical and Chemical Research. (b) Gifu College of Pharmacy. (c) Shionogi and Co., Ltd.
(2) Bencivenni, L.; Gigli, R.; Cesaro, S. N. *J. Mol. Struct.* **1979**, *53*, 25.
(3) Anzenhofer, K.; De Boer, J. J. *Z. Kristallogr.* **1970**, *131*, 103.
(4) Hazell, R. G.; Pawley, G. S.; Lund Petersen, C. E. *J. Cryst. Mol. Struct.* **1971**, *1*, 319.
(5) (a) Hoffmann, R.; Imamura, A.; Hehre, W. J. *J. Am. Chem. Soc.* **1968**, *90*, 1499. (b) Hoffmann, R.; Heilbronner, E.; Gleiter, R. *Ibid.* **1970**, *92*, 706. (c) Hoffmann, R. *Acc. Chem. Res.* **1971**, *4*, 1.
(6) Haselbach, E.; Heilbronner, E.; Schröder, G. *Helv. Chim. Acta* **1971**, *54*, 153.

0002-7863/83/1505-2172$01.50/0